Fragmentation of Protonated Peptides: Surface-Induced Dissociation in Conjunction with a Quantum Mechanical Approach

Ashley L. McCormack,† Árpád Somogyi,‡ Ashok R. Dongré, and Vicki H. Wysocki*

Department of Chemistry, Virginia Commonwealth University, Richmond, Virginia 23284-2006

This paper describes the results of a systematic investigation designed to assess the utility of surface-induced dissociation in the structural analysis of small peptides (500–1800u). A number of different peptides, ranging in mass and amino acid sequence, are fragmented by collision with a surface in a tandem mass spectrometer and the spectra are compared with data obtained by gas-phase collisional activation. The surface-induced dissociation spectra provide ample sequence information for the peptides. Side-chain cleavage ions of type w, which are generally detected upon kiloelectronvolt collisions with gaseous targets but not upon electronvolt collisions with gaseous targets, are detected in the ion–surface collision experiments. A theoretical approach based on MNDO bond order calculations is suggested for the description of peptide fragmentation. This model, supplemented by ab initio calculations, serves as a complement to the experimental work described in the paper and explains (i) the easy cleavage of the amide bond, (ii) charge-remote backbone and side-chain cleavages, and (iii) the influence of intramolecular H-bonding.

INTRODUCTION

Structural analysis of proteins and peptides by tandem mass spectrometry has progressed rapidly as an alternative or companion[1] to classical sequencing by Edman degradation. Tandem mass spectrometry is especially well-suited for mixture analysis and sequence determination of peptides with blocked N-termini, ragged C-termini, or posttranslational modifications.[1-7] With the development of matrix-assisted laser desorption ionization (MALDI)[8,9] and electrospray ionization (ESI)[10-12] there is increasing interest in obtaining structural information for large biomolecules by tandem mass spectrometry.[12-16] Both the newer (MALDI and ESI) and the traditional (fast-atom bombardment (FAB) and liquid secondary ion mass spectrometry (LSIMS))[17] ionization techniques produce protonated or multiply protonated molecules and allow molecular weight determination. To obtain unambiguous sequence information, a protonated peptide must be mass-selected by the first mass analyzer of a tandem mass spectrometer and then activated to cause fragmentation. To date, research has focused mainly on the activation and fragmentation of peptide ions by gas-phase collisions with inert target gases, specifically collision-activated dissociation (CAD) in the low- (eV) and high-energy (keV) regimes.[1-7,13-16]

Chart I

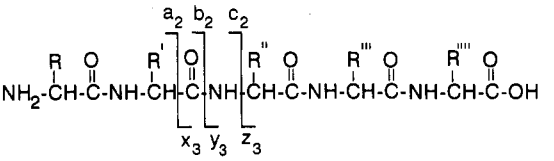

Some of the main cleavage sites for protonated peptides are shown in Chart I. The letter designations such as **b** and **y** follow a modified form[6] of the Roepstorff and Fohlman nomenclature[18] and will be used throughout this paper. The **y**-type, C-terminal ions are rearrangement ions proposed to have the general structure $^{+}H_2(HNCHRCO)_nOH$ and the **b**-type, N-terminal ions are proposed to have the general structure $H(HNCHRCO)_n^{+}$. Other peptide fragments include $\mathbf{a}_n$ ions (formally $[\mathbf{b}_n - CO]$: $H(HNCHRCO)_{(n-1)}HN{=}CHR_n^{+}$), immonium ions ($^{+}H_2N{=}CHR$), and ions corresponding to H_2O or NH_3 loss from one of the main fragment types (designated by an asterisk, e.g., a_n^*). In the MS/MS product ion spectrum, the mass difference between two adjacent ions of the same type, e.g., two adjacent **b**-type ions, specifies a mass that corresponds to an amino acid residue; this identifies the additional amino acid of the larger fragment.

Under low-energy (eV) gas-phase collision conditions compatible with quadrupole mass analyzers, dominant frag-

† Present address: Department of Molecular Biotechnology, University of Washington, FJ-20, Seattle, WA 98195.

‡ On leave from Central Research Institute for Chemistry of the Hungarian Academy of Sciences, P.O. Box 17, H-1525 Budapest, Hungary.

(1) Carr, S. A.; Hemling, M. E.; Bean, M. F.; Roberts, G. D. *Anal. Chem.* **1991**, *63*, 2802-2824.

(2) Biemann, K. In *Methods in Enzymology*; McCloskey, J. A., Ed.; Academic Press, Inc.: San Diego, CA, 1990; Vol. *193*, pp 351-360, 455-479.

(3) Yost, R. A.; Boyd, R. K. In *Methods in Enzymology*; McCloskey, J. A., Ed.; Academic Press, Inc.: San Diego, CA, 1990; Vol. *193*, pp 154-200.

(4) Gross, M. L. In *Methods in Enzymology*; McCloskey, J. A., Ed.; Academic Press, Inc.: San Diego, CA, 1990; Vol. *193*, pp 131-153.

(5) Tomer, K. B. *Mass Spectrom. Rev.* **1989**, *8*, 445-482, 483-511.

(6) Biemann, K. *Biomed. Environ. Mass. Spectrom.* **1988**, *16*, 99-111.

(7) Hunt, D. F.; Yates, J. R., III; Shabanowitz, J.; Winston, S.; Hauer, C. R. *Proc. Natl. Acad. Sci. U.S.A.* **1986**, *83*, 6233-6237.

(8) Karas, M.; Bachmann, D.; Bahr, U.; Hillenkamp, F. *Int. J. Mass. Spectrom. Ion Processes* **1987**, *78*, 53-68.

(9) Hillenkamp, F.; Karas, M.; Beavis, R. C.; Chait, B. T. *Anal. Chem.* **1991**, *63*, 1193A-1203A.

(10) Dole, M.; Mack, L. L.; Hines, R. L.; Mobley, R. C.; Ferguson, L. D.; Alice, M. B. *J. Chem. Phys.* **1968**, *49*, 2240-2249.

(11) Fenn, J. B.; Mann, M.; Meng, C. K.; Wong, S. F.; Whitehouse, C. M. *Science* **1989**, *246*, 64-71.

(12) Smith, R. D.; Loo, J. A.; Edmonds, C. G.; Barinaga, C. J.; Udseth, H. R. *Anal. Chem.* **1990**, *62*, 882-899.

(13) Smith, R. D.; Loo, J. A.; Barinaga, C. J.; Edmonds,C. G.; Udseth, H. R. *J. Am. Soc. Mass. Spectrom.* **1990**, *1*, 53-65.

(14) Smith, R. D.; Barinaga, C. J.; Udseth, H. R. *J. Phys. Chem.* **1989**, *93*, 5019-5022.

(15) Loo, J. A.; Edmonds, C. G.; Smith, R. D. *Science* **1990**, *248*, 201-204.

(16) Loo, J. A.; Edmonds, C. G.; Smith, R. D. *Anal. Chem.* **1991**, *63*, 2488-2499.

(17) Fenselau, C.; Cotter, R. J. *Chem. Rev.* **1987**, *87*, 501-512.

(18) Roepstorff, P.; Fohlman, J. *Biomed. Mass Spectrom.* **1984**, *11*, 601.

0003-2700/93/0365-2859$04.00/0

Scheme I

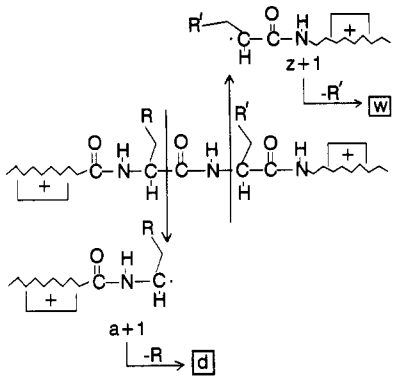

ment ion types are **b**, **y**, and immonium ions.[3,7,19-23] Under high-energy (keV) gas-phase collision conditions compatible with sector mass analyzers, the above ions are observed, as well as side-chain cleavage ions of type **d**, $H^+[H\text{-}(HNCHRCO)_{n-1}NHCH{=}CHR^o]$, and **w**, $[R^oHC{=}CHCO\text{-}(NHCHRCO)_{n-1}OH]H^+$, where R^o is the remaining substituent, if any, at the *n*th side chain (Scheme I).[2,6,19,24,25] The general appearance of high-energy and low-energy spectra are frequently different, with **a**, **d**, and **w** ions dominant in the high-energy spectra and **b** and **y** ions dominant in the low-energy spectra. The **d** and **w** ions have also been observed using collision energies greater than 300 eV with hybrid sector-quadrupole instruments.[26] Although detailed mechanistic studies have not been performed, it is generally accepted that formation of **a**, **b**, and **y** ions results from an initial bond scission adjacent to a charge site. Formation of the **d** and **w** ions is thought to be promoted by an initial bond cleavage that occurs remote from the charge site (see Scheme I and section I.3).[24,25] In Scheme I, the zig-zag lines indicate an oligopeptide chain and the charge is assumed to be located N-terminal to the cleavage site for formation of **d** ions or C-terminal to the cleavage site for formation of **w** ions. The side-chain cleavage ions are important for the differentiation of residues with the same *m/z* but different side-chain structure (e.g., leucine vs isoleucine).

Although CAD has been, and will continue to be, successfully applied to peptide sequence determination, it has been postulated that the average internal energy deposited by this activation method is insufficient to fragment large (>3500 Da) singly protonated peptides. Other approaches for the activation of polyatomic ions include photodissociation[27-32] and ion–surface collisions.[27,33-48] Surface-induced dissociation (SID), introduced by Cooks and co-workers,[33,34] can deposit high average internal energies into precursor ions and the narrow distribution of energies deposited can be shifted to lower or higher average internal energies by varying the collision energy.[34] Cooks and co-workers were the first to report peptide fragmentation by SID.[35] Several groups have since illustrated SID of peptides with a variety of different instrument designs.[34,43-48] Although these investigations demonstrated the usefulness of SID for peptide fragmentation, no systematic investigation of peptide structure determination by SID has been performed.

Here we report the results of a systematic study designed to assess the utility of SID in the structural analysis of peptides (see Table I). The focus of this investigation was to explore the fragmentation of a variety of peptides, ranging in mass and amino acid sequence, and to assess the structural information afforded by SID in comparison with the information afforded by the traditional means of fragmentation, low- and high-energy CAD. Another goal of the work was to determine whether SID produces side-chain specific sequence ions of types **d** and **w**. In addition to the experiment work, a quantum mechanical approach based on MNDO bond order calculations is presented. The main aim of this theoretical work is to determine the influence of the site of protonation on the major fragmentation pathways of model dipeptides and to determine whether MNDO bond order data are consistent with SID and CAD experimental results. For easier reading, the background and literature review for this theoretical section are given below, at the beginning of section II.

(19) Bean, M. F.; Carr, S. A.; Thorne, G. C.; Reilly, M. H.; Gaskell, S. J. *Anal. Chem.* **1991**, *63*, 1473–1481.
(20) (a) Wysocki, V. H. In *Proceedings of the NATO Advanced Study Institute on Mass Spectrometry in the Biological Sciences: A Tutorial*; Gross, M. L., Ed.; Kluwer Academic Publishers: Boston, MA, 1991; pp 59–77. (b) Hunt, D. F.; Krishnamurthy, T.; Shabanowitz, J.; Griffin, P. R.; Yates, J. R., III; Martino, P. A.; McCormack, A. L.; Hauer, C. R. In *Mass Spectrometry of Peptides*; Desiderio, D., Ed.; CRC Press: Boca Raton, FL, 1990; p 139. (c) Hunt, D. F.; Alexander, J. E.; McCormack, A. L.; Martino, P. A.; Michel, H.; Shabanowitz, J. Ed. Villafranca, J. J. In *Protein Chemistry Techniques II*; Academic Press: New York, 1991; pp 455–465. (d) Hunt, D. F.; Henderson, R. A.; Shabanowitz, J.; Sakaguchi, K.; Michel, H.; Sevilir, N.; Cox, A. L.; Appella, E.; Engelhard, V. H. *Science* **1992**, *255*, 1261–1263. (e) Hunt, D. F.; Michel, H.; Dickinson, T. A.; Shabanowitz, J.; Cox, A. L.; Sakaguchi, K.; Appella, E.; Grey, H. M.; Sette, A. *Science* **1992**, *256*, 1817–1820.
(21) Alexander, A. J.; Thibault, P.; Boyd, R. K.; Curtis, J. M.; Rinehart, K. L. *Int. J. Mass Spectrom. Ion Processes* **1990**, *98*, 107–134.
(22) Poulter, L.; Taylor, L. C. E. *Int. J. Mass Spectrom. Ion Processes* **1989**, *91*, 183–197.
(23) Ballard, K. D.; Gaskell, S. J. *Int. J. Mass Spectrom. Ion Processes* **1991**, *111*, 173–189.
(24) Johnson, R. S.; Martin, S. A.; Biemann, K.; Stults, J. T.; Watson, J. T. *Anal. Chem.* **1987**, *59*, 2621–2525.
(25) Johnson, R. S.; Martin, S. A.; Biemann, K. *Int. J. Mass Spectrom. Ion Processes* **1988**, *86*, 137–154.
(26) Alexander, A. J.; Thibault, P.; Boyd, R. K. *Rapid Commun. Mass Spectrom.* **1989**, *3*, 30–34.
(27) Castoro, J. A.; Nuwaysir, L. M.; Ijames, C. F.; Wilkins, C. L. *Anal. Chem.* **1992**, *64*, 2238–2243.
(28) Hunt, D. F.; Shabanowitz, J.; Yates, J. R., III *J. Chem. Soc., Chem. Commun.* **1987**, 548–550.
(29) Martin, S. A.; Hill, J. A.; Kittrell, C.; Biemann, K. *J. Am. Soc. Mass Spectrom.* **1990**, *1*, 107–109.
(30) Lebrilla, C. B.; Wang, D. T.-S.; Mizoguchi, T. J.; McIver, R. T., Jr. *J. Am. Chem. Soc.* **1989**, *111*, 8593–8598.
(31) Tecklenburg, R. E., Jr.; Miller, M. N.; Russell, D. H. *J. Am. Chem. Soc.* **1989**, *111*, 1161–1171.
(32) Williams, E. R.; Furlong, J. J. P.; McLafferty, F. W. *J. Am. Soc. Mass Spectrom.* **1990**, *1*, 288–294.
(33) Mabud, Md. A.; Dekrey, M. J.; Cooks, R. G. *Int. J. Mass Spectrom. Ion Processes* **1985**, *67*, 285–294.
(34) Cooks, R. G.; Ast, T.; Mabud, Md. A. *Int. J. Mass Spectrom. Ion Processes* **1990**, *100*, 209–265.
(35) Cooks, R. G.; Amy, J. W.; Bier, M. E.; Schwartz, J. C.; Schey, K.L. *Adv. Mass Spectrom.* **1989**, *11*, 33–50.
(36) Wysocki, V. H.; Ding, J.-M.; Jones, J. L.; Callahan, J. H.; King, F. L. *J. Am. Soc. Mass Spectrom.* **1992**, *3*, 27–32.
(37) (a) Winger, B. E.; Julian, R. K., Jr.; Cooks, R. G.; Chidsey, C. E. D. *J. Am. Chem. Soc.* **1991**, *113*, 8967–8969. (b) Wysocki, V. H.; Jones, J. L.; Ding, J.-M. *J. Am. Chem. Soc.* **1991**, *113*, 8969–8970.
(38) Morris, M.; Riederer, D. E., Jr.; Winger, B. E.; Cooks, R. G.; Ast, T.; Chidsey, C. E. D. *Int. J. Mass Spectrom. Ion Processes* **1992**, *122*, 181–217.
(39) Winger, B. E.; Laue, H.-J.; Horning, S. R.; Julian, R. K., Jr.; Lammert, S. A.; Riederer, D. E., Jr.; Cooks, R. G. *Rev. Sci. Instrum.* **1992**, *63*, 5613–5625.
(40) Beck, R. D.; St. John, P.; Alvarez, M. M.; Diederich, F.; Whetten, R. L. *J. Phys. Chem.* **1991**, *95*, 8402–8409.
(41) St. John, P. M.; Whetten, R. L. *Chem. Phys. Lett.* **1992**, *196*, 330–336.
(42) Somogy, Á.; Kane, T. E.; Ding, J.-M.; Wysocki, V. H. *J. Am. Chem. Soc.* **1993**, *115*, 5275–5283.
(43) Bier, M. E.; Schwartz, J. C.; Schey, K. L.; Cooks, R. G. *Int. J. Mass Spectrom. Ion Processes* **1990**, *103*, 1–19.
(44) Aberth, W. *Anal. Chem.* **1990**, *62*, 609–611.
(45) Williams, E. R.; Henry, K. D.; McLafferty, F. W.; Shabanowitz, J.; Hunt, D. F. *J. Am. Soc. Mass Spectrom.* **1990**, *1*, 413–416.
(46) Wright, A. D.; Despeyroux, D.; Jennings, K. R.; Evans, S.; Riddoch, A. *Org. Mass Spectrom.* **1992**, *27*, 525–526.
(47) Cole, R. B.; LeMeillour, S.; Tabet, J.-C. *Anal. Chem.* **1992**, *64*, 365–371.
(48) McCormack, A. L.; Jones, J. L.; Wysocki, V. H. *J. Am. Soc. Mass Spectrom.* **1992**, *3*, 859–862.

Table I. List of Peptides Investigated in This Study[a]

peptides studied (common names)	amino acid sequence[b]	$[M + H]^+$ [c] (m/z)	basic residues[d]	refs[e] SID	refs[e] CID
Leu-enkephalin	YGGFL	556		43, 44, 47	22, 47
dynorphin A 1–6	YGGFLR	712	R6		21
dynorphin A 1–7	YGGFLRR	868	R6, R7		
dynorphin A 1–9	YGGFLRRIR	1137	R6, R7, R9		21
dynorphin A 1–13	YGGFLRRIRPKLK	1603	R6, R7, R9, K11, K13		
bradykinin	RPPGFSPFR	1060	R1, R9		21
des-Arg^1-bradykinin	PPGFSPFR	903	R9		
des-Arg^9-bradykinin	RPPGFSPF	903	R1		22
lys^1-bradykinin	KPPGFSPFR	1032	R9, K1		
bradykinin 2–7	PPGFSP	583			
angiotensin III	RVYIHPF	931	R1, H5		29, 19
angiotensin I	DRVYIHPFHL	1296	R2, H6, H9	43, 46	
renin substrate	DRVYIHPFHLLVYS	1758	R2, H6, H9	45, 46	19
eledosin-related peptide	KFIGLM-NH_2	707	K1		
fibrinopeptide A	ADSGEGDFLAEGGGVR	1536	R16		
substance P	RPKPQQFFGLM-NH_2	1347	R1, K3	45	19, 25
substance P (free acid)	RPKPQQFFGLM	1348	R1, K3		22
synthetic peptide	GYLTLYKYKASA-OCH_3	1391	K7, K9		

[a] SID spectra not shown in this paper are available from the authors upon request. [b] Amino acid sequence of the peptides. Single-letter codes are used to indicate the amino acid sequence of the peptides with the amino terminus designated as position 1. [c] Monoisotopic integer mass of the protonated peptide. [d] Basic amino acids are identified by single letter codes and positions in the peptide. All peptides contain a free amino terminus. [e] Representative spectra from the literature. The list is not intended to include all published spectra for a given peptide.

EXPERIMENTAL SECTION

Materials. Peptides were obtained from Sigma (St. Louis, MO) and were used without further purification (angiotensin I, angiotensin III, bradykinin, des-Arg^1-bradykinin, des-Arg^9-bradykinin, Lys^1-bradykinin, bradykinin 2–7, leucine enkephalin, dynorphin A fragments 1–6, 1–7, 1–9, and 1–13, eledoisin-related peptide, fibrinopeptide A, substance P, substance P (free-acid form), and renin substrate). The synthetic peptide, GYLTLYKYKASA-OCH_3 was a gift from Dr. R. M., Kini, Department of Biochemistry and Molecular Biophysics, Virginia Commonwealth University, Richmond, VA.

Samples for analysis were prepared either by dissolving lyophilized peptide in 0.1% trifluoroacetic acid (Applied Biosystems, Foster City, CA) and adding a 1-μL aliquot of this solution (10–80 pmol/μL) to 3 μL of glycerol (Sigma) on a stainless steel probe tip or by dissolving lyophilized peptide directly into acidified glycerol and then adding an aliquot to the probe tip.

Mass Spectrometry. The instrument used in this investigation consists of two quadrupoles (Extrel, Pittsburgh, PA) arranged in a 90° geometry, with a surface placed to intersect the ion optical path of each quadrupole.[36] The angle of the incident beam (with respect to the surface normal) is 45–50°. The collision surfaces utilized were stainless steel or self-assembled monolayers. The covalently bound self-assembled monolayers[49] were prepared by the spontaneous assembly of octadecanethiol or 2-(perfluorooctyl)ethanethiol (mM solution in EtOH) on gold foil or vapor-deposited gold, as described recently.[37,38,42] Peptide ions were produced by liquid secondary ionization with an Antek (Palo Alto, CA) cesium ion gun operated at 6–8 keV.

To obtain single-stage mass spectra, the potential difference between the ion source and the surface was kept at approximately 0–5 V and was adjusted by varying the voltage applied to the probe tip so that the ions were transmitted past the surface without colliding with the surface. In the surface-induced dissociation experiments, the energy of the ion–surface collision (20–90 eV) was controlled by changing the potential difference between the ion formation region, determined by the voltage at the probe tip, and the surface. To maximize sensitivity, the resolution on Q1 was typically opened up to produce a parent ion envelope 3–5 amu wide. The resolution on Q2 was set to accept product ion envelopes 3–5 amu wide. This is a standard mode of operation for the related triple–quadrupole mass spectrometers that have been successfully used to sequence a large number of peptides.[7,20] Unit resolution of both precursor and product ions is possible but requires greater quantities of samples. In all cases, the instrument was tuned to maximize the ion current of a fragment ion that has a m/z approximately half that of the parent m/z, in an effort to reduce preferential collection and transmission of low-mass ions. Q2 was scanned at a rate of 150–175 Da/s over the appropriate mass range. Data were acquired and averaged with a Teknivent Vector/Two data system (Maryland Heights, MO). Peptide spectra obtained on the monolayer films at a given collision energy are highly reproducible even after several days of normal LSIMS MS/MS operation.

Collision-activated dissociation mass spectra were acquired on the Finnigan (San Jose, CA) TSQ-70 triple–quadrupole mass spectrometer as described before (2–3 m Torr, multiple–collision conditions; 20–30-eV collision energy; target gas Ar).[50] Collision-activated dissociation mass spectra recorded on the $[M + H]^+$ ions of six peptides (angiotensin III, bradykinin, Lys^1-bradykinin, and the dynorphin A 1–7, 1–9, and 1–13 fragments) were generously provided by Dr. Patrick Griffin; these spectra were acquired on a Finnigan TSQ-700 triple-quadrupole mass spectrometer by using conditions similar to those used on the TSQ-70.

RESULTS AND DISCUSSION

I. Surface-Induced Dissociation. The series of peptides investigated to assess the structural information afforded by SID are listed in Table I. Several SID spectra will be presented below to illustrate (1) the influence of *collision* energy on the extent of fragmentation and on the relative ratios of different types of ions, (2) the influence of *peptide structure* on the extent of fragmentation and the types of fragment ions that dominate the SID spectra, and (3) the appearance of **d** and **w** ions in the SID spectra. As indicated in Table I, peptides investigated range in m/z from 556 to 1758. In column 4 of Table I we highlight the locations of basic groups in the peptides because the location of basic group is known[19,25] to influence the types of fragment ions observed when other activation methods are used. When possible, our SID spectra

(49) (a) Laibinis, P. E.; Whitesides, G. M.; Allara, D. L.; Tag, Y.-T.; Parikh, A. N.; Nuzzo, R. G. *J. Am. Chem. Soc.* **1991**, *113*, 7152–7167. (b) Finklea, H. O.; Hanshew, D. D. *J. Am. Chem. Soc.* **1992**, *114*, 3173–3181. (c) Bryant, M. A.; Pemberton, J. E. *J. Am. Chem. Soc.* **1991**, *113*, 3629–3637.

(50) Erikson, A. K.; Payne, D. M.; Martino, P. A.; Rossomando, A. J.; Shabanowitz, J.; Weber, M. J.; Hunt, D. F.; Sturgill, T. W. *J. Biol. Chem.* **1990**, *265*, 19728–19735.

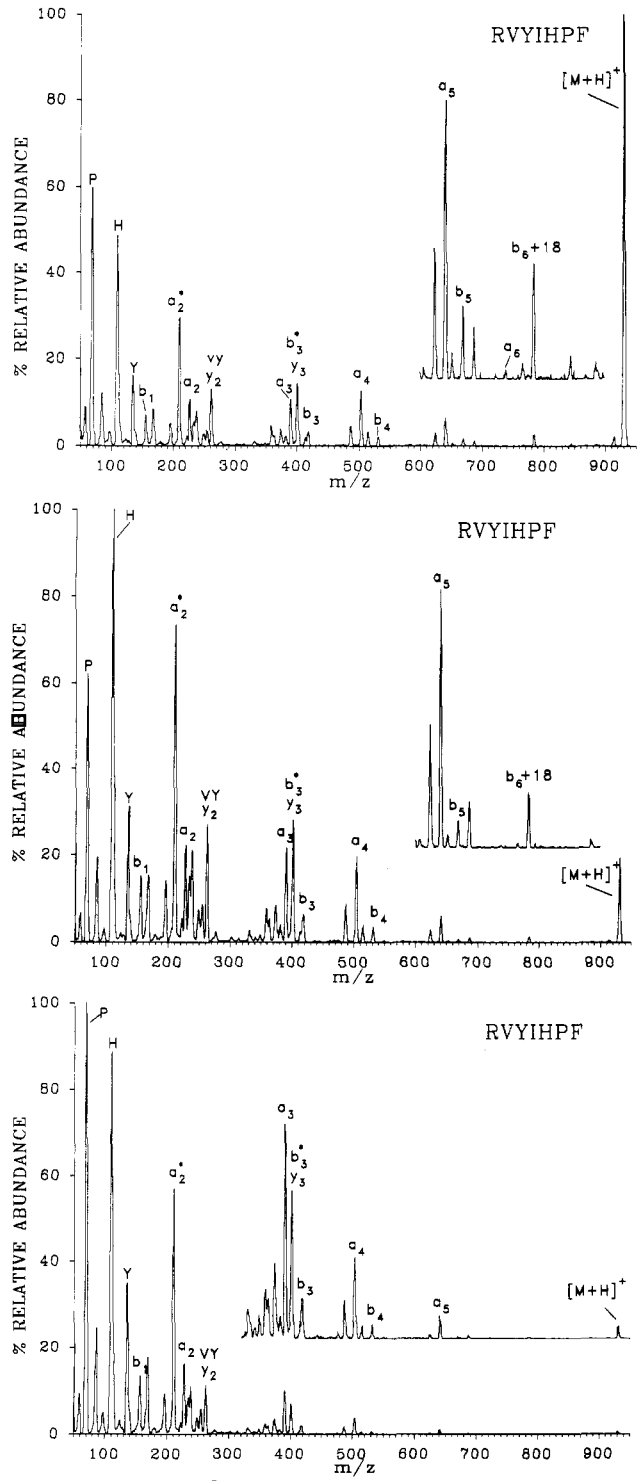

Figure 1. Surface-induced dissociation spectra of the $[M + H]^+$ ion (m/z 931) of angiotensin III (RVYIHPF) at collision energies of (a, top) 30, (b, middle) 50, and (c, bottom) 70 eV on an octadecanethiolate ($CH_3(CH_2)_{17}SAu$) monolayer surface.

are compared with published spectra obtained by SID in other laboratories, as well as with spectra obtained by low- and high-energy CAD experiments. However, comparisons made between spectra obtained on different types of instruments (CAD vs SID; sector vs hybrid vs quadrupole) must be interpreted with caution because experimental conditions can affect the relative abundances detected for CAD and SID; e.g., a given instrument may be operated in a manner that discriminates against low-mass ions.

1. Influence of Collision Energy on Observed Fragmentation. It has been illustrated that the *average* internal energy that can be deposited is higher for SID than for low- and high-energy CAD.[34,51] It has also been shown that the internal energy deposited by SID varies in a controllable fashion with collision energy and that the amount of energy deposited at a given collision energy depends on the surface and projectile ion involved.[34,38,42] To assess the effect of collision energy on the SID spectra of singly charged peptides, each of the peptides listed in Table I was studied by using at least two different collision energies, within the range of 20–70 eV. Panels a–c of Figure 1 show the 30-, 50-, and 70-eV SID spectra of the $[M + H]^+$ ion, m/z 931, from angiotensin III. As with smaller molecules[34] and large cluster ions,[40,41] the energy transferred to peptides in the SID process is easily varied. A series of ions of type **a** and **b** are present in each spectrum of Figure 1, and the sequence RVYXHPF is afforded (where X stands for leucine or isoleucine). The presence of both **b** and **a** ions simplifies sequencing for an unknown, because **a**:**b** pairs are readily identified by their 28-Da mass difference. Our SID spectra are similar to CAD spectra that we obtained by using low-energy collisions and to CAD spectra published by Bean and co-workers.[19] In the 30-eV SID spectrum, three low-mass product ions, immonium ions of proline, histidine, and tyrosine, represent ca. 28% of the total ion current and the parent ion is about 15% of the total ion current. As the collision energy is increased to 70 eV, the total intensity of these three immonium ions increases to 47% of the total ion current, while the parent decreases to less than 0.1% of the total ion current. The decrease in relative abundance of the parent ion suggests that at higher energies fewer parents are withstanding the surface collision.

The ratio $\mathbf{a}_n$:$\mathbf{b}_n$ may serve as another measure of the variation of internal energy as a function of collision energy, because **a** ions can be formed by loss of CO from **b** ions. For instance, as shown in Figure 1a and c, the ratio $\mathbf{a}_3$:$\mathbf{b}_3$ observed in the SID spectra of angiotensin III increases from 3 to 6 as the collision energy is increased from 30 to 70 eV. A similar trend was observed for most of the peptides investigated. In general, the relative abundance of low-mass fragment ions increases with increasing collision energy and the parent ion abundance decreases with increasing collision energy.

The 50- and 70-eV SID spectra of the $[M + H]^+$ ion of a larger peptide, fibrinopeptide A (m/z 1536), are shown in panels a and b of Figure 2, respectively. The series of **b**-type ions allows the assignment of residues 3–5 and 8–9; the series of **y**-type ions allow the assignment of residues 1–4 and 6–16. (The **w** ions indicated with boxed labels are discussed below.) The amino acid sequence ADSGEGDFLAEGGGVR is afforded by both spectra. At 50-eV collision energy, three immonium ions which correspond to the amino acids arginine, leucine, and phenylalanine are only 9% of the total ion current and the parent ion represents 33% of the total ion current. At 70-eV collision energy, these immonium ions increase to 15% of the total ion current, and although the base peak corresponds to the precursor ion, it represents only 7% of the total ion current.

Cole et al. have recently examined the energy dependence of the SID spectra of a number of smaller peptides.[47] They showed that the kinetic energy spread produced in the parent ion population by the FAB ionization technique directly influences low-energy SID spectra. We have observed the same effect for the larger peptides investigated here; i.e., a large variety of different ion types are observed even at low apparent kinetic energies. However, our experiments show that the kinetic energy spread from the ionization method has a decreasing influence as the collision energy increases. A source-induced kinetic energy spread of 5 eV is more important for 20-eV collisions than for 70-eV collisions, for

(51) (a) DeKrey, M. J.; Kenttämaa, H. I.; Wysocki, V. H.; Cooks, R. G. *Org. Mass. Spectrom.* **1986**, *21*, 193–195. (b) Wysocki, V. H.; Kenttämaa, H. I.; Cooks, R. G. *Int. J. Mass Spectrom. Ion Processes* **1987**, *75*, 181–208. (c) Kim, M. S.; McLafferty, F. W. *J. Am. Chem. Soc.* **1978**, *100*, 3279–3282.

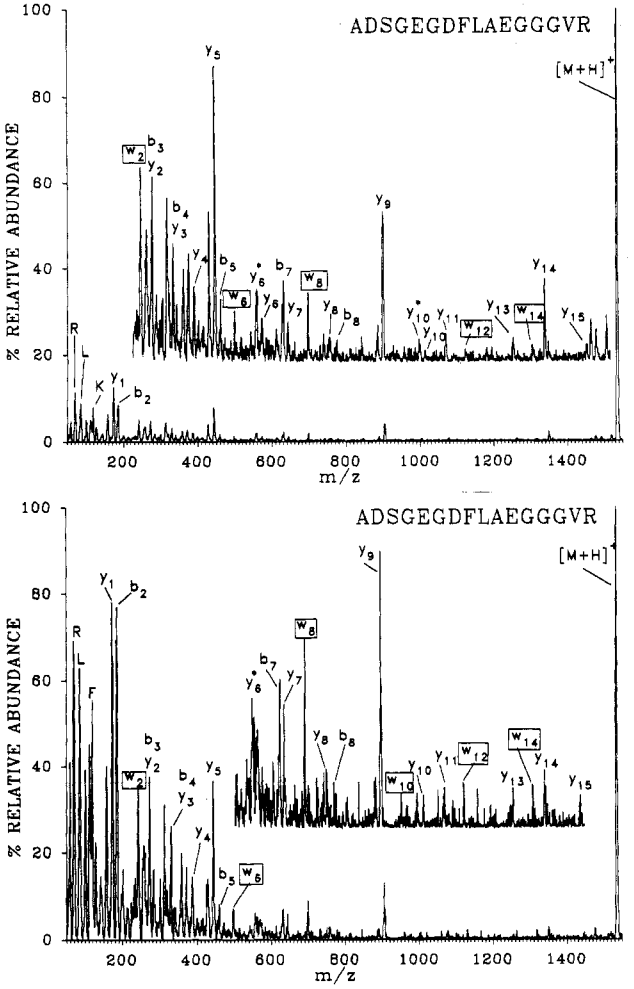

Figure 2. Surface-induced dissociation spectra of the $[M + H]^+$ ion (m/z 1536) of fibrinopeptide A (ADSGEGDFLAEGGGVR) at collision energies of (a, top) 50 and (b, bottom) 70 eV on an octadecanethiolate ($CH_3(CH_2)_{17}SAu$) monolayer surface. Labels for w ions shown in boxes.

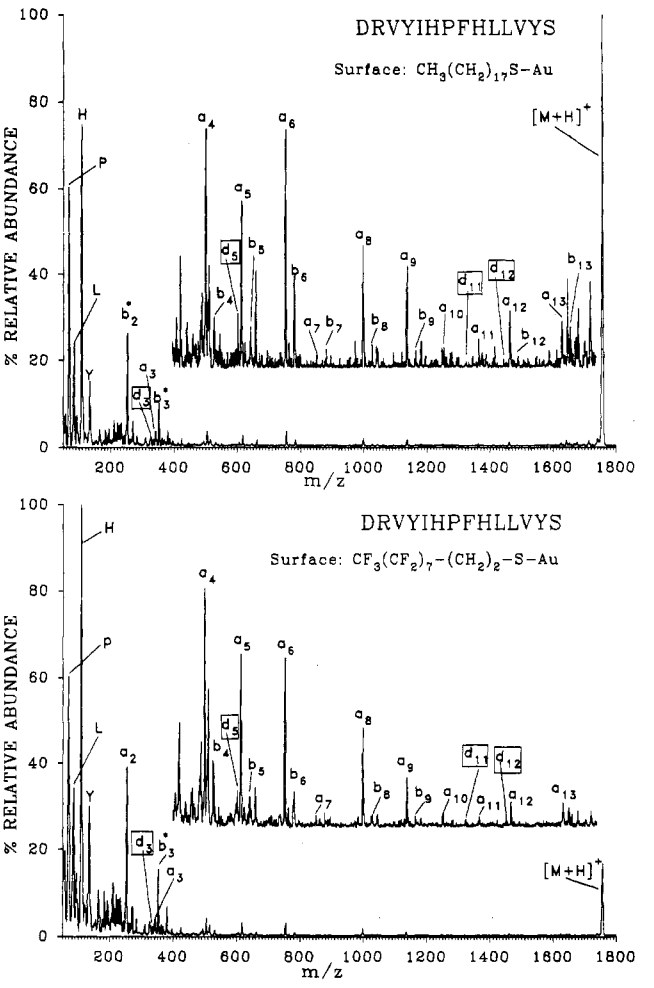

Figure 3. Surface-induced dissociation spectra of the $[M + H]^+$ ion (m/z 1758) of renin substrate (DRVYIHPFHLLVYS) at collision energies of 50 eV on (a, top) octadecanethiolate ($CH_3(CH_2)_{17}SAu$) and (b, bottom) 2-(perfluorooctyl)ethanethiolate ($CF_3(CF_2)_7CH_2CH_2SAu$) monolayer surfaces. In both cases, the quantity of sample loaded on the probe tip was 80–100 pmol.

example, and collision energies higher than those used by Cole[47] are required to fragment the large, arginine-containing peptides in Table I. We are currently examining the influence of the LSIMS kinetic energy distribution, as well as the *internal* energy distribution, on the SID spectra by comparing the LSIMS-SID results with those for which the ions are produced by the "cooler" electrospray ionization technique (ESI/SID). Our preliminary SID data, at a given SID energy, show a significantly decreased extent of fragmentation for ions produced by ESI in comparison with those formed by LSIMS.

Although the influence of the nature of the surface was not a subject of this investigation, a comment on this is appropriate because the variation of the surface type is another way to vary the internal energy deposition. Figure 3 shows the 50-eV SID spectra for collisions of the $[M + H]^+$ ion of renin substrate (m/z 1758) with self-assembled monolayer films prepared from octadecanethiol (Figure 3a) and 2-(perfluorooctyl)ethanethiol (Figure 3b). More extensive fragmentation is observed for the fluorinated surface, as illustrated by the less intense parent ion, $[M + H]^+$ and by the increased $\mathbf{a}_6$:$\mathbf{b}_6$ ratio (Figure 3). These results are consistent with those obtained for molecules other than peptides and are in line with the interpretation of the earlier results: the fluorinated alkanethiolate surface behaves as a "harder" surface and the alkanethiolate surface behaves as a "softer", more deformable surface.[38,39,42] This means that less energy is deposited into the surface (vibrational) modes for the fluorinated surface, and therefore, a larger portion of the kinetic energy of the projectile is transformed into *ion* internal energy.

2. Influence of Peptide Structural Features on Observed Fragmentation. The number and locations of basic groups in a peptide influence the appearance of the SID spectra. Peptides with no arginine, for example, fragment extensively at low collision energies and yield both **b** and **y** ions. The results obtained for a synthetic peptide provided to us as an unknown illustrate this point. The peptide was thought to have the structure GYLTLYKYKASA (MW = 1377). However, the mass spectrum of ions produced by LSIMS showed a major peak at m/z 1391, suggesting the presence of an additional CH_2 in the synthetic peptide. SID gave a complete series of **b** ions at a collision energy of only 10 eV and led to the conclusion that the methyl ester of the peptide was the product actually synthesized (GYLTLYKYKASA-OCH_3). Other data are consistent with this conclusion. The $\mathbf{y}_1$–$\mathbf{y}_{11}$ series of ions, for example, are shifted by 14 u, confirming the C-terminus as the site of modification. In addition, no shift in m/z of the $[M + H]^+$ ion was observed in the LSIMS spectrum after the sample was subjected to esterification conditions. Comparison of the SID spectra of a number of peptides has shown that peptides with arginine at the amino terminus are likely to produce a **b** (or **a**) series that is more dominant than the **y** series (see, for example, Figures 1 and 3). In contrast, peptides with arginine at the carboxy terminus yield, in addition to **a**, **b**, and immonium ions, product ions that contain the carboxy terminus (see ions $\mathbf{y}_n$ and $\mathbf{w}_n$ in Figure 2 and figures presented below). These results are in agreement with CAD results.

The internal energy deposited into protonated peptides by different activation methods is known to be less effective for inducing fragmentation with increasing mass of the peptide.[13-16,52,53] We found no direct and unambiguous correlation between the size of the peptides in Table I and the fragmentation efficiency. It should, however, be remembered that the dependence of the SID spectra on the mass of the peptides listed in Table I is complicated by the fact that increases in size are accompanied by changes in the sequences of the peptides, and the sequence influences the dissociation, as described above. Furthermore, this mass dependence is not necessarily the same for SID and CAD, and additional studies with a polymeric amino acid, e.g., $(Ala)_n$, are required. In this case, a more reliable comparison could be made with the theoretical prediction reported recently for $(Ala\text{-}Gly)_n$ (n = 2–800) systems.[53]

3. Side-Chain Specific Sequence Ions. In high-energy CAD spectra, Johnson and co-workers[24,25] noted ions that involve loss of the substituent at the β-carbon atom of the peptide side chain (backbone carbon designated α). They suggested that the formation of these **d** and **w** ions involves the pathway shown in Scheme I: charge-remote homolytic cleavage, followed by radical-induced cleavage at the β,γ bond of the terminal amino acid [$(\mathbf{a}_n + 1 - R \rightarrow \mathbf{d}_n$; $(\mathbf{z}_n + 1) - R' \rightarrow \mathbf{w}_n$]. They also showed that the formation of these **d** and **w** product ions is sequence dependent.[24,25] Ions of type **d** are formed if a basic residue is located at either the N-terminus or "N-terminal" to the cleavage site of the peptide, and ions of type **w** are formed if a basic residue is located at either the C-terminus of the peptide or "C-terminal" to the cleavage site. Leucine enkephalin (YGGFL), for example, is not expected to produce **d** or **w** ions because it has no basic residues, while dynorphin fragment 1–6 (YGGFLR) is expected to produce a $\mathbf{w}_2$ ion. Some amino acids do not give rise to **d** or **w** ions because homolytic cleavage of a CH_2–aryl bond would be required (e.g., phenylalanine, tyrosine, tryptophan), no side chain is present (glycine), or no γ-carbon is present (alanine). Interestingly, the structure of proline does permit the formation of ions of type **w**. In this case, homolytic cleavage of the N–C backbone bond occurs without dissociation of the ion and is followed by cleavage of the β,γ bond.[24,25] Ions of type **d** and **w** can be used to differentiate the structural isomers leucine and isoleucine,[2,19,24,25] and the appearance of these ions in high-energy CAD spectra is often presented as an advantage of multisector instruments over triple–quadrupole instruments. It should be noted that predicted **d** or **w** ions are not always observed even in high-energy CAD spectra.[2,24,25]

It has been suggested that charge-remote fragmentations of ions occur at relatively high gas-phase collision energies, especially those available in the high-energy regime.[2,19,22,24-26,54] The process has also been detected at low collision energies for a number of surfactants,[26,55,56] although charge-remote fragmentation of peptides has not been studied in detail using low-energy gas-phase collisions. In general, ions of type **d** and **w** are not reported under low-energy multiple-collision conditions; nevertheless, Alexander and co-workers have shown side-chain specific sequence ions can be produced by using 300-eV collisions (laboratory frame) with argon (multiple-collision conditions).[26]

(52) (a) Uggerud, E.; Derrick, P. J. *J. Phys. Chem.* **1991**, *95*, 1430–1436. (b) Demirev, P.; Olthoff, J. K.; Fenselau, C.; Cotter, R. J. *Anal. Chem.* **1987**, *59*, 1951–1954.

(53) Griffin, L. L.; McAdoo, D. J. *J. Am. Soc. Mass Spectrom.* **1993**, *4*, 11–15.

(54) (a) Jensen, N. J.; Tomer, K. B.; Gross, M. L. *J. Am. Chem. Soc.* **1985**, *107*, 1863–1868. (b) Adams, J. *Mass Spectrom. Rev.* **1990**, *9*, 141–186.

(55) Wysocki, V. H.; Ross, M. M. *Int. J. Mass Spectrom. Ion Processes* **1991**, *104*, 179–211.

(56) Wysocki, V. H.; Bier, M. E.; Cooks, R. G. *Org. Mass. Spectrom.* **1988**, *23*, 627–633.

Table II. List of Peptides Studied; Residues for Which d or w Ions Are Expected[a] and Observed[b]

ions of type d	ions of type w
	YGGF*L*R
	YGGF***L***R
YGGFLRRIR	YGGF***LRRI***R
YGGFLRRIRPKLK	YGGF***LRRI***RPK***L***K
RVYIHPF	
DRVYIHPFHL	
DRVYIHPFHL***LV***YS	
RPPGFSPFR	R***PP***GF***S***PFR
KPPGFSPFR	K***PP***GFS***P***FR
RPKPQQFFGLM-NH_2	
RPKPQQFFGLM	
	AD***S***G***E***G***D***F***L***A***E***GGG***V***R
GYLTLYKYKASA-OMe	GYL***T***L***Y***KYKASA-OMe

[a] Residues underlined for which **d** or **w** ions are expected. [b] Residues bold, italicized, and underlined for which **d** or **w** ions are observed.

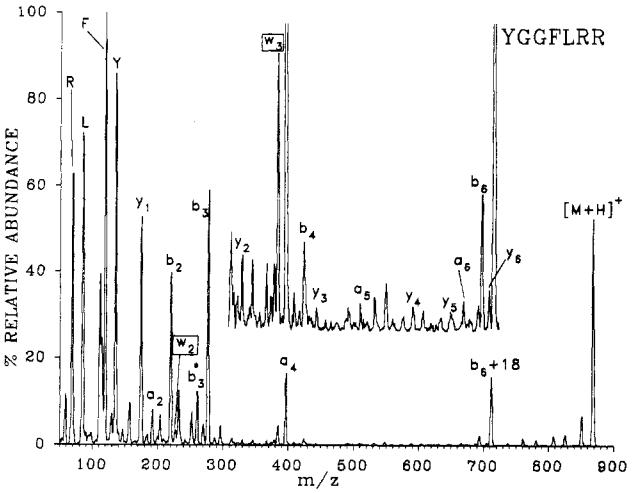

Figure 4. Surface-induced dissociation spectrum of the $[M + H]^+$ ion (m/z 868) of dynorphin A 1–7 (YGGFLRR) at a collision energy of 50 eV on an octadecanethiolate ($CH_3(CH_2)_{17}SAu$) monolayer surface.

With surfactant molecules, ions resulting from charge-remote fragmentation have been reported in surface-induced dissociation spectra.[56] In the present work, an investigation was undertaken to determine if ion–surface collisions produce side-chain specific sequence ions from protonated peptides. The series of related peptides listed in Table II were chosen in order to track the **d** and **w** ions as the peptide structure changes. The residues that are predicted to give side-chain-specific ions are underlined and those that actually exhibit side-chain specific sequence ions in SID spectra are also shown in bold-face type. An examination of Table II shows that ions of type **d** are observed for only a few of the peptides investigated. One difficulty encountered in searching for these ions is that many of the predicted **d** ions overlap with other fragments, making assignment of particular ions as **d** ions somewhat ambiguous. Nevertheless, in the SID spectra of renin substrate (Figure 3), the $\mathbf{d}_{11}$ and $\mathbf{d}_{12}$ ions can be assigned, because they do not overlap with other ions. In general, SID spectra exhibit ions of type **w** (see, for examples, Figures 2, 4, and 5 and Table II). In Figure 2b, for example, peaks for $\mathbf{w}_{14}$, $\mathbf{w}_{12}$, $\mathbf{w}_{10}$, $\mathbf{w}_8$, $\mathbf{w}_6$, and $\mathbf{w}_2$ are all present, and in Figure 4 peaks for $\mathbf{w}_3$ and $\mathbf{w}_2$, the only expected **w** ions, are present. Note that, at the SID collision energies investigated here (20–70 eV), the **w** ions are not as abundant as those found in high-energy CAD spectra and the **w** ions increase in relative abundance as the internal energy deposited into the proto-

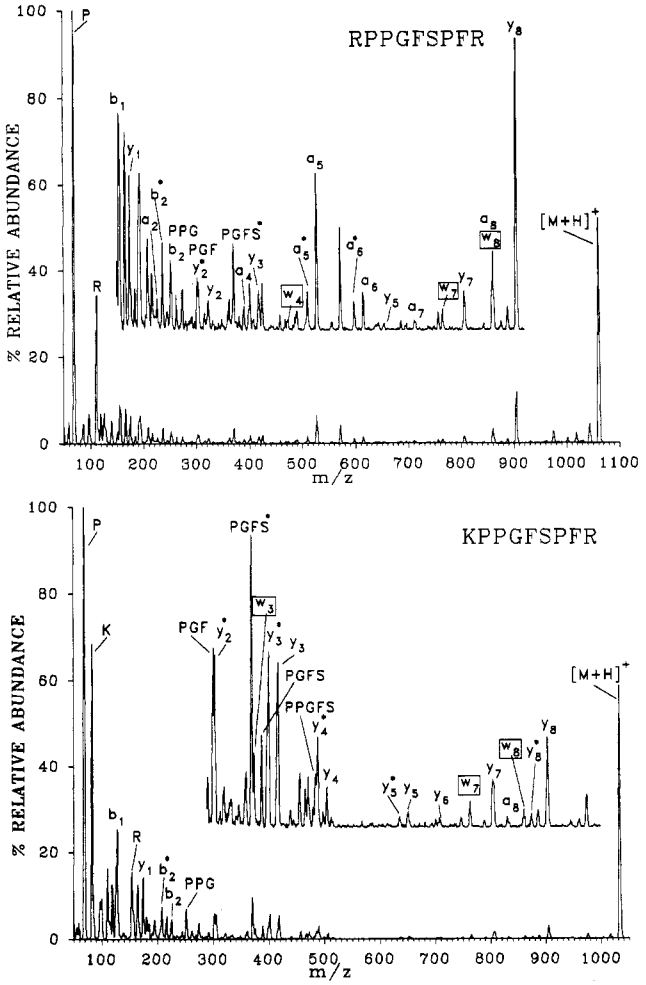

Figure 5. Surface-induced dissociation spectrum of (a, top) the $[M + H]^+$ ion (m/z 1060) of bradykinin (RPPGFSPFR) at a collision energy of 50 eV on an octadecanethiolate ($CH_3(CH_2)_{17}SAu$) monolayer surface and (b, bottom the $[M + H]^+$ ion (m/z 1032) of Lys^1-bradykinin (KPPGFSPFR) at collision energy of 50 eV on an octadecanethiolate ($CH_3(CH_2)_{17}SAu$) monolayer surface. In (b) only those segments are indicated that can be assigned from the spectra.

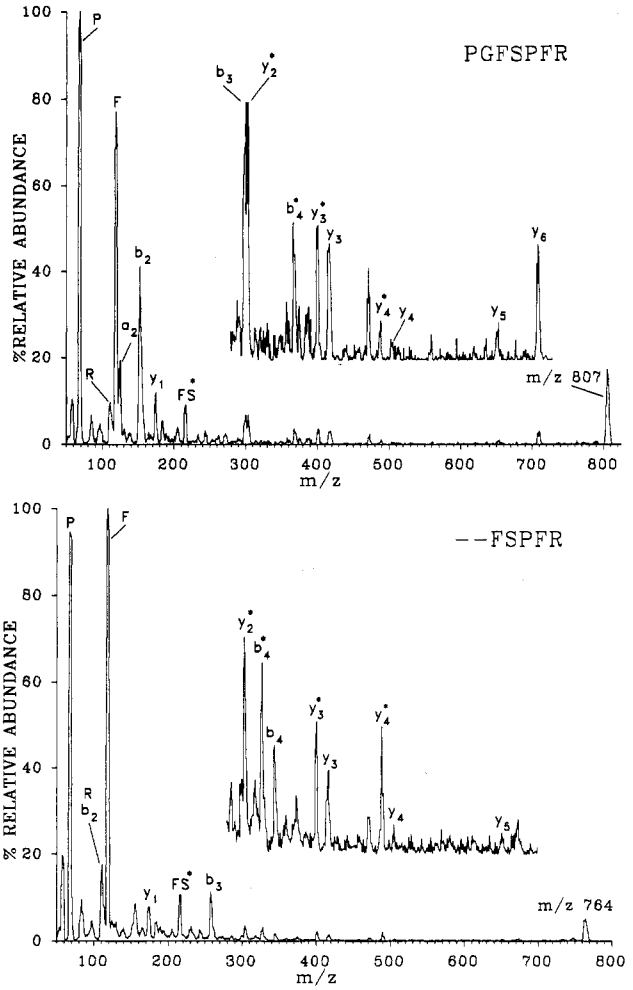

Figure 6. Surface-induced dissociation spectrum of the ions (a, top) m/z 807 and (b, bottom) 764 formed by LSIMS of bradykinin. The spectra were obtained at a collision energy of 40 eV on an octadecanethiolate ($CH_3(CH_2)_{17}SAu$) monolayer surface.

nated peptide increases (i.e., by changing the SID collision energy or surface type).

Figure 5a shows the 50-eV SID spectrum recorded on the $[M + H]^+$ ion, m/z 1060, of bradykinin (RPPGFSPFR). The spectrum shows ions at m/z 764 and 861, labeled $\mathbf{w}_7$ and $\mathbf{w}_8$, respectively, which result from cleavage of the proline side chain. The peaks corresponding to $\mathbf{w}_8$, m/z 861, and $\mathbf{a}_8$, m/z 858, may overlap at the resolution used to obtain this spectrum, SID of the related peptide, Lys^1-bradykinin (KPPGFSPFR) also produces ions at m/z 764 and 861 (Figure 5b), which further confirms that these ions are $\mathbf{w}_7$ and $\mathbf{w}_8$; i.e., replacement of arginine with lysine at the amino terminus should not cause a mass shift for ions that contain the C-terminus of the peptide. (Note that $\mathbf{a}_8$ does not overlap with $\mathbf{w}_8$ in this case.) Research by Johnson and co-workers using a tandem sector instrument showed that the internal energy deposited during ionization by fast-atom bombardment is sufficient to produce side-chain specific sequence ions.[24,25] Our LSIMS single-stage mass spectrum of bradykinin showed fragment ions at m/z 764 and 807. We selected these ion source fragments of bradykinin as "unknowns" for SID to confirm their identity as **w** and **y** ions and to lend support to the claim that the ions of the same m/z in the SID spectrum of bradykinin are also **w** and **y** ions. The 40-eV SID spectrum recorded for the ion at m/z 807 is shown in Figure 6a. A series of ions of type **y** and **y*** (y-NH_3) are present in the spectrum and the spectrum affords the sequence PGFSPFR; the structure of this ion thus corresponds to $\mathbf{y}_7$. A series of **b**-type ions confirms the assignments for residues 1–4. For comparison, Figure 6b shows the 40-eV SID spectrum recorded on the ion at m/z 764. Note that the series of **y**-type ions have not shifted in m/z; however, the **b**-type ion series have shifted. This spectrum affords the sequence FSPFR and is thus consistent with the structure proposed for the $\mathbf{w}_7$ ion. The formation of side-chain cleavage ions will be further considered in section II.

II. Quantum Chemical Investigation. As discussed above, CAD and SID spectra exhibit "sequence-specific" fragmentation; i.e., the appearance or absence of selected fragment ion types can be related to the position of basic groups, such as arginine.[12–14,22–26,57,58] Although investigators are beginning to consider the role of the protonation site(s) on fragmentation of peptides,[6,25,57–62] no systematic investigation has been performed that definitively reveals the effect

(57) Burlet, O.; Orkiszewski, R. S.; Ballard, K. D.; Gaskell, S. J. *Rapid Commun. Mass Spectrom.* **1992**, *6*, 658–662.
(58) Tung, X.; Boyd, R. K. *Rapid Commun. Mass Spectrom.* **1992**, *6*, 651–657.
(59) (a) Mallis, L. M.; Russell, D. H. *Anal. Chem.* **1986**, *58*, 1076–1080. (b) Russell, D. H.; McGlohon, E. S.; Mallis, L. M. *Anal. Chem.* **1988**, *60*, 1818–1824.
(60) Grese, R. P.; Cerny, R. L.; Gross, M. L. *J. Am. Chem. Soc.* **1989**, *111*, 2835–2842. (b) Leary, J. A.; Zhou, Z.; Ogden, S. A.; Williams, T. D. *J. Am. Soc. Mass Spectrom.* **1990**, *1*, 473–480. (c) Teesch, L. M.; Adams, J. *J. Am. Chem. Soc.* **1991**, *113*, 812–820.
(61) (a) Wagner, D. D.; Salari, A.; Gage, D. A.; Leykam, J.; Fetter, J.; Hollingsworth, R.; Watson, J. T. *Biol. Mass Spectrom.* **1991**, *20*, 419. (b) Watson, J. T.; Wagner, D. S.; Chang, Y.-S.; Strahler, J. R.; Hanash, S. M.; Gage, D. A. *Int. J. Mass Spectrom. Ion Processes* **1991**, *111*, 191–209.
(62) Yeh, R. W.; Grimley, J. M.; Bursey, M. M. *Biol. Mass Spectrom.* **1991**, *20*, 443–450.

of the proton location on bond cleavages. Based on experimental results, several mechanisms for the formation of characteristic peptide fragment ions have been proposed.[6,23,25,57,63-65] In general, the formation of these ions is assumed to be triggered by protonation on the amide nitrogen,[25] but protonation on the terminal amino group[62] has also been suggested. The proton affinity values of the important amino acids and polyglycines are available;[66] however, these measurements cannot give us unambiguous information about the site of protonation of a fragmenting peptide. In addition to work on protonated peptides, it has been shown that ms/ms spectra of metal ion adducts of peptides provide useful structural information.[60,67]

Another approach to the description of peptide fragmentation, the application of theoretical (e.g., *quantum mechanical*) methods, is less popular, probably because a "small" peptide is too "large" for high-level calculations (e.g., even for a single configuration, self-consistent-field, Hartree–Fock (SCF) ab initio calculation). This is a severe limitation mainly when one wants to determine *energetics* of protonation or fragmentation with reliable accuracy. Relatively high level ab initio calculations can only be used for simple models or amino acids, e.g., acetamide[68] and glycine.[67,69a] (Note, however, that ab initio methods are more frequently used for studies of neutral peptide conformations,[69] and it has been shown that high-level calculations are necessary to describe reliably the conformers[69a-c] and electrostatic interactions[69d] of amino acids and peptides.)

It is known that other inherent and informative parameters besides the *energy* of a system can also be calculated from the quantum mechanical wave function. These parameters, which provide a link between quantum mechanics and "classical" chemistry, include *charge densities*, *valencies* on the individual atoms of a molecule (*free valencies* in open-shell systems), and *bond orders* between different atoms in a chemical species. A priori, there are different ways to define these quantities (for details see, for example, refs 70–72 and references therein), and rigorously, only those which are calculated according to the same definitions can be compared. It has been illustrated that Mulliken–Mayer[71,72] bond orders and valencies can be successfully applied for the prediction of gas-phase ion structures and primary mass spectral fragmentation processes[73] (for more detailed examples, see the papers on oxazolones,[74,75] norbornanes,[76,77] 1,3-cyclodisiloxanes,[78,79] diboranes,[80] and cyclopropylsilanes[81]). The results cited above show that, although bond orders cannot be regarded as *reactivity* indexes, the bonds preferred for fragmentation in molecular ions are those for which the calculated bond orders are *significantly smaller* than in the corresponding neutrals. In spite of the criticism of the semiempirical method MNDO[82] for the calculation of *energetics*,[67a] several examples have recently been shown by Somogyi et al.[75,80] where the MNDO *bond indexes* were close to those determined by ab initio calculations (e.g., STO-3G and 6-31G** SCF). It has also been found that fine details for geometries have no significant effect on the calculated bond orders.[80]

Chart II

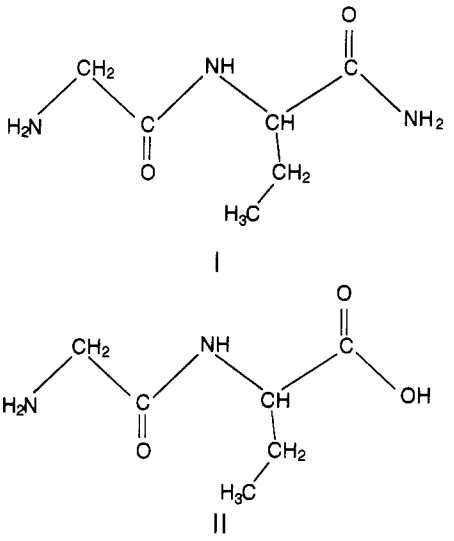

In this work, MNDO calculations have been carried out on two model compounds, **I** and **II** (Chart II), their singly protonated forms, and some neutrals and ions (types **b**, **a**, **a** + 1, **y**, **z**, and **z** + 1) derived from these structures. Ab initio calculations have also been performed for selected ions and neutrals. Geometries were completely optimized in each case. The goal of the calculations is to investigate the effect of the site(s) of protonation on the main fragmentation processes of peptides, especially on the cleavage of the amide bond. This is accomplished by using MNDO bond orders to characterize bond strengthening and bond weakening due to protonation on various heteroatoms in the model "peptides" **I** and **II**. Charge-remote fragmentation pathways are also addressed. To simplify the discussion below, the backbone atoms of **I** and **II** are numbered 1–7, starting at the amino terminus (e.g., the amide nitrogen of residue 2 is referred to as N_2; see Figure 7).

1. MNDO Bond Orders in Neutral and Protonated Peptides. MNDO bond orders calculated for bonds between heavy atoms in the model compounds **I** and **II** and for their

(63) (a) Cordero, M. M.; Boyle, S. V.; Wesdemiotis, C. *Proceedings of the 40th ASMS Conference on Mass Spectrometry and Allied Topics*, Washington, DC, 1992; pp 41–42. (b) Wesdemiotis, C.; Polce, M. J.; Cai, J.; Baranovo, S. *Ibid* pp 43–44.

(64) Cordero, M. M.; Houser, J. J.; Wesdemiotis, C. *Anal. Chem.*, in press.

(65) Kenny, P. T. M.; Nomoto, K.; Orlando, R. *Rapid Commun. Mass Spectrom.* **1992**, *6*, 95–97.

(66) (a) Meot-Ner, M.; Hunter, E. P.; Field, F. H. *J. Am. Chem. Soc.* **1979**, *101*, 686–689. (b) Locke, M. J.; McIver, R. T., Jr. *J. Am. Chem. Soc.* **1983**, *105*, 4226–4232. (c) Bojesen, G. *J. Am. Chem. Soc.* **1987**, *109*, 5557–5558. (d) Gorman, G. S.; Speir, J. P.; Turner, C. A.; Amster, I. J. *J. Am. Chem. Soc.* **1992**, *114*, 3986–3988. (e) Wu, Z.; Fenselau, C. *J. Am. Soc. Mass Spectrom.* **1992**, *3*, 863–866.

(67) (a) Jensen, F. *J. Am. Chem. Soc.* **1992**, *114*, 9533–9537. (b) Bouchonnet, S.; Hoppilliard, Y. *Org. Mass Spectrom.* **1992**, *27*, 71.

(68) Wong, M. W.; Wiberg, K. B. *J. Phys. Chem.* **1992**, *96*, 668–671.

(69) (a) Császár, A. G. *J. Am. Chem. Soc.* **1992**, *114*, 9568–9575. (b) Schäfer, L.; Newton, S. Q.; Cao, M.; Peeters, A.; Van Alsenoy, C.; Wolinski, K.; Momany, F. A. *J. Am. Chem. Soc.* **1993**, *115*, 272–280. (c) Perczel, A.; McAllister, M. A.; Császár, P.; Csizmadia, I. G. *J. Am. Chem. Soc.* **1993**, *115*, 4849–4858. (d) Price, S. L.; Andrews, J. S.; Murray, C. W.; Amos, R. D. *J. Am. Chem. Soc.* **1992**, *114*, 8268–8276.

(70) Giambiagi, M.; de Giambiagi, M. S.; Grempel, D. R.; Heynmann, C. D. *J. Chim. Phys.* **1975**, *72*, 15–22.

(71) Mayer, I. *Chem. Phys. Lett.* **1983**, *97*, 270–274; **1985**, *117*, 396.

(72) Mayer, I. *Int. J. Quantum Chem.* **1986**, *29*, 73–84; **1986**, *29*, 477–483.

(73) Somogyi, Á.; Gömöry, Á.; Vékey, K.; Tamás, J. *Org. Mass Spectrom.* **1991**, *26*, 936–938.

(74) Curcuruto, O.; Traldi, P.; Cativiela, C.; Diaz de Villegas, M. D.; Garcia, J. I.; Mayoral, J. A.; Ajo, D. *J. Heterocycl. Chem.* **1990**, *27*, 1495–1499.

(75) Császár, A. G.; Somogyi, Á.; Pócsfalvi, G.; Traldi, P. *Org. Mass Spectrom.* **1992**, *27*, 1349–1356.

(76) Curcuruto, O.; Favretto, D.; Traldi, P.; Ajo, D.; Cativiela, C. Mayoral, J. A.; Lorez, M. P.; Fraile, J. M.; Garcia, J. I. *Org. Mass Spectrom.* **1991**, *26*, 977–984.

(77) Gömöry, Á.; Somogyi, Á.; Tamás, J.; Stájer, G.; Bernáth, G.; Komáromi, I. *Int. J. Mass Spectrom. Ion Processes* **1991**, *107*, 225–246.

(78) Somogyi, Á.; Tamás, J. *J. Phys. Chem.* **1990**, *94*, 5554–5556.

(79) Somogyi, Á.; Tamás, J.; Császár, A. G. *J. Mol. Struct. THEOCHEM* **1991**, *232*, 123–131.

(80) Somogyi, Á.; Gömöry, Á. *Chem. Phys. Lett.* **1992**, *192*, 221–228.

(81) Vékey, K.; Somogyi, Á.; Tamás, J.; Pócsfalvi, G. *Org. Mass Spectrom.* **1992**, *27*, 869–875.

(82) Dewar, M. J. S.; Thiel, W. *J. Am. Chem. Soc.* **1977**, *99*, 4899–4907.

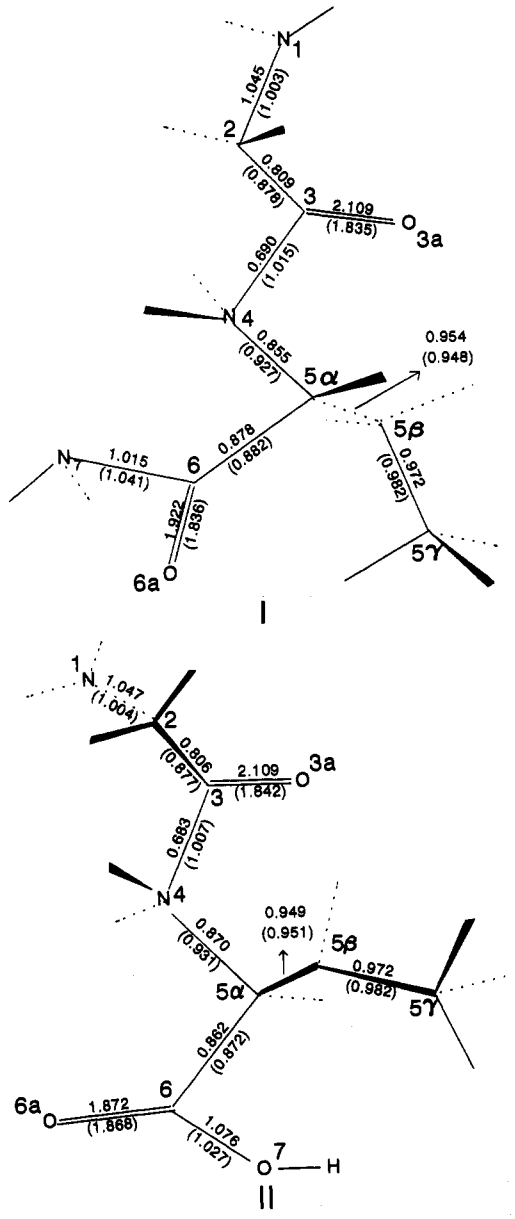

Figure 7. MNDO bond orders and the numbering of heavy atoms in the amide N_4-nitrogen protonated and neutral (in parentheses) forms of model compounds I and II.

singly protonated forms are collected in Table III. For simplicity, the carbon–hydrogen, nitrogen–hydrogen, and oxygen–hydrogen bond orders are omitted; their values are very close to unity and only slightly affected by the protonation. For easier comparison, bond order data obtained for the N_4 protonated forms of **I** and **II** and the corresponding neutrals are also shown in Figure 7, with data for the neutrals shown in parentheses. It is worth mentioning that the data given in Table III and shown in Figure 7 are almost independent of the nature of the terminal groups, $CONH_2$ (**I**) or COOH (**II**).

Bond orders in the neutral molecules are quite close to the "classically" expected values of 1 and 2 for single and double bonds, respectively.[83] As far as the different protonated forms are concerned, it can be concluded from the data in Table III that, in general, bond orders for bonds remote from the charge site remain practically unchanged after protonation (compare the $C_{5\alpha}$–C_6 value in the neutral molecule with the $C_{5\alpha}$–C_6

(83) Although "simple" molecular ions ($M^{\bullet+}$) are not formed in FAB ionization, it is interesting to note that in such hypothetical molecular ions the carbon–carbon bonds neighboring to the amide carbonyl group (i.e., bonds $C_{5\alpha}$–C_6 and C_2–C_3 in I and II, respectively) are calculated to be considerably weaker than in the corresponding neutrals (Table III).

Table III. MNDO Bond Orders between Heavy Atoms in the Model Peptides I and II (M), their Molecular Ions, ($M^{\bullet+}$), and Monoprotonated Forms Designated by the Location of the Proton[a]

bond	neutral molecule M	protonated forms N_4	N_1	X_7	O_{3a}	O_{6a}	molecular ion $M^{\bullet+}$
I							
N_1—C_2	1.003	1.045	0.888	1.023	1.042	1.015	1.026
C_2—C_3	0.878	0.809	0.874	0.866	0.831	0.865	0.908
C_3=O_{3a}	1.835	2.109	1.801	1.832	1.236	1.861	1.957
C_3—N_4	1.015	0.690	1.121	0.967	1.493	0.952	0.843
N_4—$C_{5\alpha}$	0.927	0.855	0.885	0.964	0.855	0.969	1.105
$C_{5\alpha}$—$C_{5\beta}$	0.948	0.954	0.953	0.943	0.950	0.945	0.931
$C_{5\beta}$—$C_{5\gamma}$	0.982	0.972	0.978	0.979	0.975	0.979	0.977
$C_{5\alpha}$—C_6	0.882	0.878	0.881	0.834	0.876	0.846	0.631
C_6=O_{6a}	1.836	1.922	1.882	2.117	1.840	1.271	1.875
C_6—N_7	1.041	1.015	1.022	0.687	1.076	1.437	1.150
II							
N_1—C_2	1.004	1.047	0.884	1.015	1.046	1.016	1.209
C_2—C_3	0.877	0.806	0.877	0.862	0.824	0.861	0.575
C_3=O_{3a}	1.842	2.109	1.849	1.845	1.240	1.871	1.907
C_3—N_4	1.007	0.683	1.072	0.957	1.484	0.936	1.122
N_4—$C_{5\alpha}$	0.931	0.870	0.910	0.971	0.860	0.980	0.876
$C_{5\alpha}$—$C_{5\beta}$	0.951	0.949	0.951	0.941	0.944	0.944	0.947
$C_{5\beta}$—$C_{5\gamma}$	0.982	0.972	0.978	0.978	0.975	0.978	0.976
$C_{5\alpha}$—C_6	0.872	0.862	0.869	0.822	0.864	0.817	0.857
C_6=O_{6a}	1.868	1.872	1.809	2.139	1.876	1.362	1.872
C_6—O_7	1.027	1.076	1.078	0.596	1.061	1.304	1.058

[a] The numbering scheme for the atoms is shown in Figure 7.

values of the protonated forms N_4, N_1, and O_{3a}). This suggests that bond order values for derivatized peptides with a fixed site of charge[61] or with a basic arginine residue are approximated by the values for the neutral (for all bonds removed from the charge site by >3 bonds). The bond order values for the neutral model compounds may thus be useful for the prediction of charge-remote fragmentation in protonated peptides. For instance, the weakest bonds in the neutral molecules **I** and **II** (lowest calculated bond orders) are the carbon–carbon bonds of the backbone (e.g., C_2–C_3 and $C_{5\alpha}$–C_6) and preferred cleavage of these bonds can be assumed.[73-81] This cleavage would lead either to an **a** + 1 ion if the remote charge is on the amino terminal portion of the peptide or to a "pseudo" **z** + 1 ion if the remote charge is on the carboxy terminus, with the pseudo **z** + 1 ion defined as [OCNH···(**z** + 1)]. As will be shown below, MNDO bond orders and energetic considerations are consistent with formation of these ions as precursor ions of **d** and **w** ions, respectively. Note that direct cleavages producing **z** + 1 ions would require cleavage of the backbone bond that has the next lowest bond order, compared with the C–C backbone bonds (e.g., cleavage of a bond such as N_4–$C_{5\alpha}$, with a bond order of 0.927 in the neutral **I**, would lead directly to a **z** + 1 ion for a peptide with a proton located at the (remote) C-terminal end of the molecule).

Protonation on the amide nitrogen (N_4) leads to a significant decrease in the C_3–N_4 amide bond order (ca. 30%, from 1.015 to 0.690 for model **I**, and from 1.007 to 0.683 for model **II**; Figure 7). It can, therefore, be assumed that the cleavage of the amide bond is preferred energetically for these protonated forms. As was mentioned above, only two other nearby bonds, C_2–C_3 and N_4–$C_{5\alpha}$, have significantly lower bond order values in the N_4-protonated forms than in the neutrals (by only about 10%; Figure 7). The significant decrease of the amide bond order in the case of the amide N protonation (N_4) is in excellent agreement with the experimental results reported recently by Wesdemiotis et al.[63b] On the basis of CAD and neutralization–reionization (NR) experiments, they suggested a preferred cleavage of the amide bond in the simplest protonated amide, formamide.

The protonation of terminal nitrogens (N_1 and N_7 in **I** and N_1 in **II**) and terminal oxygen (O_7 in **II**) leads to the weakening

of the corresponding connecting bonds [N_1–C_2 and C_6–X_7, X = N (I) or O (II)], which is not surprising. This weakening, however, is much more pronounced in the vicinity of the C=O (group X_7 protonation) than at the CH_2 group (N_1 protonation). It is also evident that protonation on carbonyl oxygen atoms (O_{3a}, O_{6a}) causes significant weakening of the original double C=O bond. From the point of mass spectral fragmentation, it is much more important that the adjacent amide bond orders are considerably larger than in the corresponding neutrals, by ca. 40–50% for both models I and II. For another comparison, the corresponding amide bond order values (C_3–N_4) are 1.493 for protonation at the oxygen O_{3a} and 0.690 for protonation at nitrogen N_4 in the case of model compound I. These bond orders are also in agreement with the length of the amide bond calculated by Wiberg et al. for acetamide,[68] and by us for O- and N-protonated acetamide. Higher level ab initio geometry optimizations (at the Hartree–Fock level, using the 6-31G** basis set) showed that the amide C–N bond length is significantly *longer* (1.557 Å) in the N-protonated form, while *shorter* (1.293 Å) in the O-protonated form than that calculated for the neutral[68] acetamide (1.356 Å). This trend in the amide bond orders (and bond lengths) means that even if the protonation is preferred on the carbonyl oxygen atom, it is of low probability that the amide bond is cleaved in these forms, i.e., that the formation of the **b**, **y** and **a** ions takes place from these amide O-protonated forms. In other words, our MNDO bond order calculations suggest that the cleavage of the amide bond is much more preferred in the amide nitrogen protonated forms, although fragmentation pathways that involve carbonyl oxygen protonated forms cannot be absolutely excluded. This does not mean that only the amide N and O are protonated or that fragmentation occurs only from these forms, as will be discussed under Conclusions.

The established "local" effect of protonation encourages us to say that calculations on larger model compounds would not affect significantly the main conclusions given in this work. Of course, this does not mean that *quantum mechanical* calculations on extended-size oligopeptides could not give us additional information. Important questions can, for instance, be posed: what are the effects of bridged, H-bonded structures which can be formed in larger peptides, specific configurations that may result from certain local sequences in large peptides, or specific conformations formed by addition of a proton or a metal ion?[60,67]

2. H-Bonded Structures. Starting with the MNDO optimized geometry of the N_4-amide nitrogen-protonated form of compound I, the ab initio STO-3G SCF calculation led to a N_4···H···N_7 H-bonded structure. We calculated the MNDO bond orders for this "bridged" form, and the data are shown in Figure 8. The two N···H bonds were calculated to have a bond order close to 0.5, which shows the usefulness of bond orders in the description of hydrogen bonds, too. It is seen in Figures 7 and 8 that even in this H-bonded form the amide bond orders (C_3–N_4 and C_6–N_7) are lower than those found in the neutral, with the greatest effect at theC_3–N_4 amide bond. Therefore, it can be assumed that formation of N···H···N bonds makes the amide bonds the preferred sites for primary bond cleavage. Although not shown here, we note that hydrogen bridge forms such as N_1···H···O_{3a} in I and O_{3a}···H···O_{6a} in II lead to bond orders significantly higher than unity for the C_3–N_4 amide bond. A general conclusion can, therefore, be drawn; N···H···N type hydrogen bonds decrease, while O···H···O types increase, the amide C(O)–N bond order.

3. Additional Notes on the Formation of b, a, y, z, d, and w Ions. As we mentioned above, bond order values cannot be considered as reactivity indexes; therefore, they cannot be used *directly* for the description of bond cleavages. From this respect, the heats of reactions leading to different

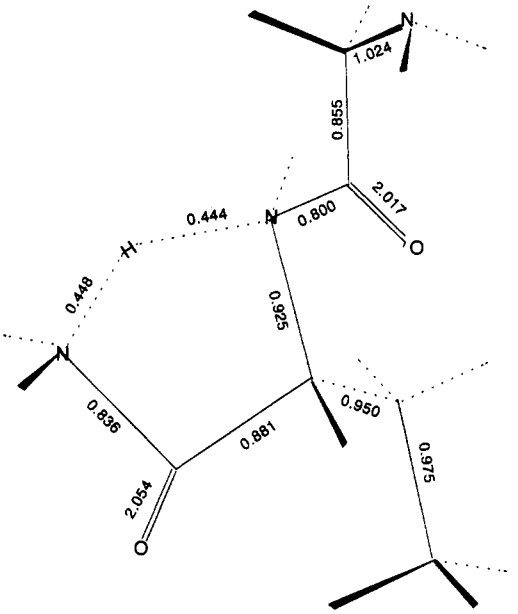

Figure 8. MNDO bond orders obtained at the STO-3G optimized geometry of the N_4···H···N_7 hydrogen-bond form of compound I.

types of fragment ions could be more relevant. The comparison of these energetic data to each other (for competitive processes) and to the corresponding bond order values also provides useful information. Knowing the limited accuracy of MNDO heats of formation, we restrict ourselves to the description of *qualitative trends* in simple bond cleavages and also use energetic results obtained by higher level ab initio calculations for comparison with the *semiempirical* data. MNDO heats of formation of the model compounds I and II, their singly protonated forms, and selected ionic and neutral fragments are given in Table IV.

In accordance with the very low amide bond order in the N_4-protonated form (0.690 for I; Figure 7), the formation of a **b**-type ion is a preferred process energetically. This simple bond cleavage leading to the $\mathbf{b}_1$ ion ($[H_2NCH_2CO]^+$) and the corresponding neutral fragment is predicted to be endothermic by the MNDO method by only 10.8 kcal/mol for model I and only 7.6 kcal/mol for model II. (For the loss of CO from the $\mathbf{b}_1$ and $\mathbf{b}_2$ ions, see below.) For the same N_4 nitrogen-protonated model compound (see reaction 1), the simple

$$\mathbf{b}_1 + NH_2CH(C_2H_5)C(O)XH \leftarrow NH_2CH_2C(O)\overset{C_3-N_4}{\downarrow}-NH_2^+-\overset{N_4-C_{5\alpha}}{\downarrow}CH(C_2H_5)C(O)XH \rightarrow NH_2CH_2CONH_2 + \mathbf{z}_1 \quad (1)$$

homolytic bond cleavage (N_4–$C_{5\alpha}$) leading to the $\mathbf{z}_1$ ion [$[CH(CH_2CH_3)COX]^+$, X = NH_2 (I) and OH (II)] and the corresponding neutral fragment was calculated to be more endothermic than formation of $\mathbf{b}_1$ by C_3–N_4 cleavage (by approximately 30 kcal/mol). This is in agreement with what is observed experimentally and with the calculated bond orders. That is, the bond order for the N_4–$C_{5\alpha}$ bond is larger (0.855 for I; Figure 7, Table III) in the N_4-protonated form than that of the amide C_3–N_4 bond (0.690 for I). Therefore, at least qualitatively, a good agreement was found between the bond order values and the thermochemistry of the *primary* bond cleavages; the reaction enthalpies increase with increasing bond orders.

Formation of the y Ion. The formation of a **y** ion involves a rearrangement reaction. On the basis of the CAD experiments on $[(Ala)_nH^+]$ (n = 2, 3, 4)[63a,64] and on deuterated [(GGGAA)H^+],[65] it was suggested recently that in the formation of the **y** ions a hydrogen is transferred not from the neighboring carbon but the adjacent amide nitrogen

Table IV. MNDO Heats of Formation, ΔH_f (kcal/mol), of Model Compounds I and II, Their Molecular Ions, Their Protonated Forms, and Selected Model Fragments

		ΔH_f I	ΔH_f II
Neutral Molecules			
M		-81.7	-130.8
Molecular Ions			
$M^{\bullet+}$		140.8	100.0
Protonated Forms[a]			
N_4		105.3	59.1
N_1		91.4	41.9
X_7		90.8	57.8
O_{3a}		80.7	37.9
O_{6a}		78.4	34.5
Model Fragments[b]			
from I and II			
$H_2N{=}CH_2^+$	a_1	186.8	
$H_2NCH_2CO^+$	b_1	164.2	
$H_2NCH(C_2H_5)COX'$		-48.1	-97.5
$H_2NCH_2CONHCH(C_2H_5)^+$	a_2	138.5	
$H_2NCH_2CONHCH(C_2H_5)CO^+$	b_2	121.9	
[cyclo-$NHCOCH_2$] (A)[c]		6.4	
$H_2NCH{=}C{=}O$ (B)[c]		4.3	
$^+H_3NCH(C_2H_5)COX'$	y_2	121.4	79.2
$H_2NCH_2CONH_2$		-37.9	
$^+CH(C_2H_5)COX'$	z_1	182.2	133.2
$OCNHCH(C_2H_5)C(OH)_2^+$		80.2	
$CH(C_2H_5)C(OH)_2^+$	$z+1$	88.2	
from leucine model[b,d]			
$^+H_3NCH_2CONHCHCH_2CH(CH_3)_2$	a_2+1	145.7	
$H_2NCH_2CONHCHCH_2CH(CH_3)_2$		-32.0	
$^+H_3NCH_2CONHCH{=}CH_2$	d_2	154.4	
$^{\bullet+}CH_2CONHCHCH_2CH(CH_3)_2$	$(a_2+1)^*$	158.4	
$^+(HO)_2CCHCH_2CH(CH_3)_2$	z_1+1	82.8	
small neutral fragments			
CH_2NH_2		19.3 (37.0)[e]	
$CH(CH_3)_2$		1.5 (16.8)[e]	
NHCO		-9.1 (-25)[e]	
CO		-6.2 (-26.4)[e]	
NH_3		-6.3 (-11.0)[e]	

[a] The numbering of atoms is given in Figure 7. X_7 denotes N and O in species I and II, respectively. [b] ΔH_f values for ionic fragments and complementary neutrals are given, X' denotes NH_2 and OH in species I and II, respectively. [c] See Chart III for structures, and ref 85 for MP2 6-31G**//6-31G** SCF energies. [d] In this model, the C_2H_5 model side chain is replaced by the $CH_2CH(CH_3)_2$ side chain of leucine. [e] Values in parentheses are experimental heats of formation.

Chart III

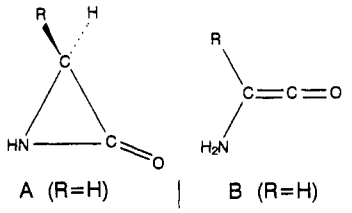

located N-terminal to the cleavage site. This means that the neutral species formed in this fragmentation process initially has an aziridinone structure,[65,65,84] cyclo-[HNCH(R)CO] (structure **A**, Chart III), rather than the isomeric aminoketene, $H_2NC(R){=}C{=}O$ (structure **B**, Chart III). Our calculations for the analogous structures of the product neutrals of **I** predict structure **B** (R = H) to be *more stable* than **A** (R = H) by

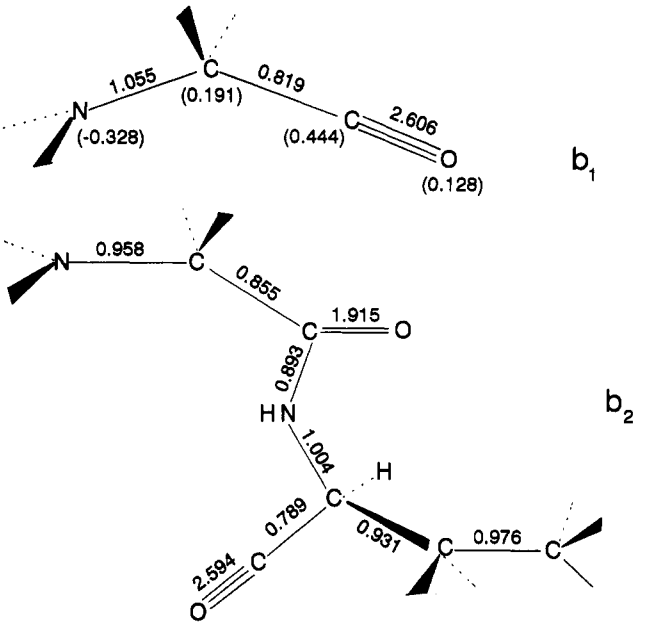

Figure 9. MNDO bond orders for two **b** ions, which can be formed from protonated forms of the model peptides I and II. Net charge densities on heavy atoms of b_1 are given in parentheses.

2.1 (MNDO) and 3.5 kcal/mol [ab initio, at the second-order Møller–Plesset perturbation theory (MP2), MP2 6-31G**//6-31G** SCF level].[85] Although these quantum mechanical predictions are seemingly in disagreement with the CAD experiments, it should be taken into account that the transition state leading to the thermodynamically more stable $H_2NCH{=}C{=}O$ product presumably has a "tight" four-membered-ring structure, rather than a "loose" five-membered structure. Kinetically, the five-membered-ring transition state would prevail, in agreement with the experimental results.

Formation of a Ions from b Ions. One mechanism for the formation of **a** ions is loss of CO from **b** ions. Because the heat of formation of CO is overestimated by the MNDO method, the experimental heat of formation of CO was used in reaction enthalpy calculations for the formation of **a** ions from **b** ions. In addition, we carried outMP2 6-31G**//6-31G** SCF ab initio calculations for the loss of CO from the model $\mathbf{b}_1$ ion. The loss of CO from the **b** ions is calculated to be exothermic by both methods [MNDO predictions are -3.8 and -9.8 kcal/mol for $\mathbf{b}_1 \rightarrow (\mathbf{a}_1 + CO)$ and $\mathbf{b}_2 \rightarrow (\mathbf{a}_2 + CO)$, respectively; the MP2 6-31G**//6-31G** SCF prediction[86] is -12.6 kcal/mol for the former process]. Accordingly, the MNDO bond orders for the bond between the carbonyl C and the adjacent carbon atom are 0.819 ($\mathbf{b}_1 \rightarrow \mathbf{a}_1 + CO$) and 0.789 ($\mathbf{b}_2 \rightarrow \mathbf{a}_2 + CO$) as illustrated in Figure 9. These values are less than unity by about 20%, and they are consistent with the above order of exothermicity. Note that the high bond order values of ca. 2.6 for the carbonyl carbon–oxygen bond are in good agreement with the "classical", triple-bond structure for the carbonyl group in the **a** ion (Figure 9). Similar MNDO bond order values were obtained recently in the open-ring oxazolone molecular ion, and the loss of CO from the open-ring molecular ion was also predicted to be slightly exothermic by ab initio calculations.[75]

Side-Chain Cleavages. As was mentioned above, cleavage of the weakest C–C bonds of the backbone can lead to **a** + 1 and pseudo **z** + 1 [OCNH···(z + 1)] ions, if the remote charge is located on the amino and carboxy termini, respectively. Although **a** + 1 ions are not generally detected in

(84) Mueller, D. R.; Eckersley, M.; Richter, W. J. *Org. Mass Spectrom.* **1988**, *23*, 217–222.

(85) MP2 6-31G**//6-31G** SCF total energy values: E_{tot}(A) = -207.338 735 hartree, E_{tot}(B) = -207.344 326 hartree. All ab initio calculations were performed by using the program package GAMESS: Schmidt, M. W.; Baldridge, K. K.; Boatz, J. A.; Jensen, J. H.; Koseki, S.; Gordon, M. S.; Nguyen, K. A.; Windus, T. L.; Elbert, S. T. GAMESS, *QCPE Bull.* **1990**, *10*, 52–54.

(86) MP2 6-31G**//6-31G** total energy values: $NH_2CH_2CO^+$, E_{tot} = -207.688 7946 hartree; $CH_2NH_2^+$, E_{tot} = -94.690 796 hartree; CO, E_{tot} = -113.018 033 hartree.

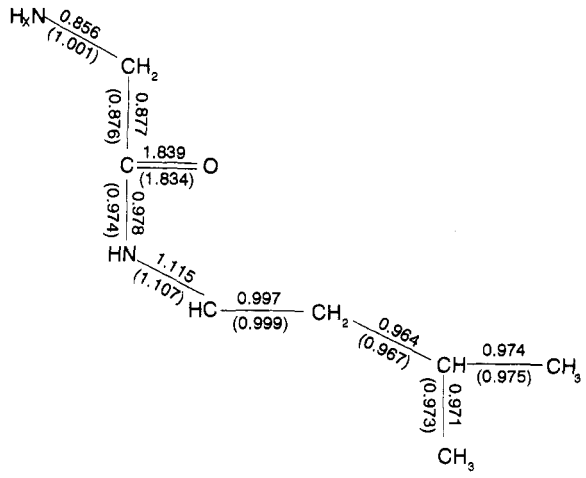

Figure 10. MNDO bond orders in an **a** + 1 model ion (x = 3) and in its corresponding neutral radical (x = 2; values in parentheses). The group $CH_2CH(CH_3)_2$ represents the leucine side chain.

MS/MS experiments, Biemann and co-workers have shown that **a** + 1 ions fragment by H loss to produce **a** ions and by cleavage at the side chain to produce **d** ions; **a** and **d** ions are often strong in kiloelectronvolt CAD spectra.[25] The substitution of the side-chain C_2H_5 in model compounds **I** and **II** by $CH_2CH(CH_3)_2$ leads to a model which contains a leucine residue and allows us to estimate the energy of formation of a **d** ion from an **a** + 1 ions. In our model "**a** + 1" ion, the charge was located on the terminal amino group, although, as can be seen in Figure 10, the charge has no significant effect on the calculated bond orders in the vicinity of the radical site. This means that this model could describe "charge-remote" side-chain cleavages, where the proton is thought to reside on a remote basic side chain. Relatively high ca. 0.96, Figure 10) bond orders calculated for the C_β–C_γ bond suggest that the C_β–C_γ side-chain cleavage, i.e., the loss of $CH(CH_3)_2$, is a high-energy cleavage and it would be only slightly favored over cleavage of any of the adjacent C–C or C–N bonds. The heat of this reaction was calculated to be 25.5 kcal/mol (by using the experimental heat of formation of the isopropyl radical and MNDO heats of formation; Table IV). This energy is in addition to the heat of reaction for formation of the $\mathbf{a}_n$ + 1 ions, which requires a (presumably energetic) simple cleavage of the backbone C–C bond (see the discussion above for the neutral models). Overall, the heat of reaction for the charge-remote formation of a **d** ion is thus predicted to be significantly larger than that calculated for the amide bond cleavage from the amide N_4-protonated form (Figure 7). Both bond order and energetic data are in good agreement with experimental observations; the formation of **d** ions is observed mainly in high-energy CAD experiments. We note that the heat of a competitive process, the loss of NH_3 from the "**a** + 1" ion of Figure 10 is predicted to be only slightly endothermic (by 1.7 kcal/mol, using the experimental heat of formation of NH_3 and MNDO heats of formation; Table IV). Easy NH_3 loss is also predicted by bond order values (see Figure 10) *and* has been investigated experimentally by Schey and co-workers,[87] who showed that the $\mathbf{a}_2$ + 1 ion from pentaalanine fragments by loss of NH_3. The competitive loss of NH_3 from the amino terminus is, of course, not expected from a "true" **a** + 1 ion where the charge resides on a remote basic site chain; i.e., the values for the neutral model shown in parentheses in Figure 10 probably provide a better model for the **a** + 1 ions described by Biemann.[25]

We suggested in section II.1 that side-chain cleavage ions of type **w** may be formed by a three-step process that involves

(87) Thornburg, K. R.; Schey, K. L.; Knapp, D. R. *J. Am. Soc. Mass Spectrom.* **1993**, *4*, 424–427.

Scheme II

Formation of w ions

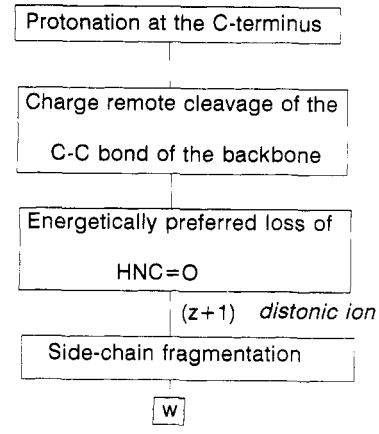

homolytic cleavage of the backbone bonds with the lowest bond order [C–C(O) bonds], loss of HN=C=O from the pseudo **z** + 1 ion, and then side-chain cleavage (Scheme II). Direct formation of a **z** + 1 ion (Scheme I)[25] may also occur and would require cleavage of the backbone N–C bond.[88] It is reasonable to assume that the energy required for the cleavage of the C–C(O) bond of the backbone is not affected significantly by the charge location of the remote charge (amino vs carboxy terminus). Thus, the formation of a pseudo **z** + 1 ion, such as modeled by the structure in Figure 11a, could be a high-energy,[88] but real process. MNDO bond order data (Figure 11a) indicate that in this structure the NHCO is loosely bound to the rest of the ion; the C–N bond order is significantly less than unity. Therefore, the loss of NHCO from this ion is predicted to be energetically favorable. (The loss of NHCO from this ion is predicted to be slightly exothermic by the MNDO method, ΔH_r = –3.5 kcal/mol.) This process leads to the formation of a **z** + 1 ion, which is presumably vibrationally excited. In these ions, as modeled by the structures in Figure 11b,c, the "side-chain" C–C bond has a lower bond order than other C–C bonds. These values (0.913 and 0.922, respectively) are slightly smaller than that obtained for the same bond in the **a** + 1 model (0.964; Figure 10). This, together with the easy loss of NHCO, suggests that the formation of the **w** ions via this pathway (Scheme II) would be slightly more favored energetically than the formation of the **d** ions via **a** + 1 precursors. This is in accordance with the SID results: more **w** than **d** ions are observed in ion–surface collision spectra. Fragmentation of an excited **z** + 1 ion (Scheme II) to yield a **w** ion is also in agreement with the production of $\mathbf{w}_n$ ions from **z** + 1 ions in reaction intermediate scans "even in the absence of added collision gas", as reported recently by Gaskell and co-workers.[89] It is also of interest that free valence values clearly indicate the distonic character of the **z** + 1 ion; as expected classically, the highest free valence value (0.577) is located on the CH carbon atom (Figure 11) and not on the atoms of the $C(OH)_2$ group, on which most of the net charge is located.

The general absence of **d** and **w** ions in low-energy CAD spectra (15–50 eV, multiple-collision conditions)[19] suggests

(88) It is difficult to estimate the relative order of the energetics of the C–C(O) and N–C bond cleavages based on MNDO heats of formation. The MNDO method overestimates the heat of formation of HNCO (Stewart, J. J. P. *J. Comput. Chem.* **1989**, *10*, 221–264), thus the heat of formation of $OCNH\cdots CH(C_2H_5)C(OH)_2$ ion could also be overestimated. However, if one relies on MNDO energetic data, the cleavage of these bonds is predicted to be endothermic by about 3 eV. Unfortunately, higher levels of ab initio calculations to get more reliable energetic data for these bond cleavages were computationally prohibitive.

(89) Ballard, K. D.; Gaskell, S. J. *Proceedings of the 41th ASMS Conference on Mass Spectrometry and Allied Topics* 1993, San Francisco, in press.

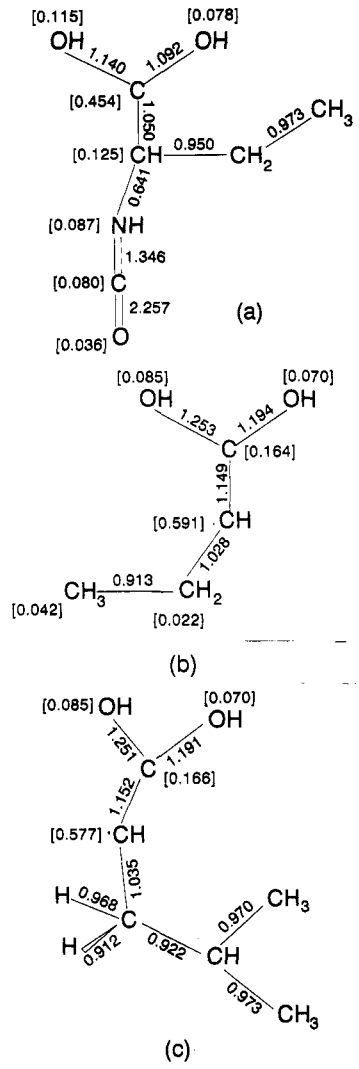

Figure 11. MNDO bond orders and free valences in (a) a pseudo **z** + 1 model ion, (b) a **z** + 1 model ion obtained by the NHCO loss from the structure (a), and (c) an analogous model ion, in which the side chain is modeled for a leucine segment. Free valences are in brackets.

that these fragmentations have relatively high internal energy requirements or that the fragmentation is influenced by the manner in which the energy is deposited (stepwise vs single step). The bond order values and SID results suggest that both of these factors contribute. Although the *average* internal energy deposited during low-energy multiple gas-phase collisions can be higher than the average energy deposited during low-energy single collisions and high-energy gas-phase collisions, this average internal energy is deposited during many collisions and the energy deposited per collision is lower. Consequently, competitive fragmentation reactions which have low internal energy requirements, such as rearrangements, may proceed before enough internal energy is deposited for higher energy decompositions to occur, resulting in low-energy CAD spectra with few **d** or **w** ions. In contrast, high-energy CAD produces a percentage of ions with internal energies much higher[51] than the average internal energy and these higher energy ions could be the source of the **d** and **w** product ions. SID, at the collision energies investigated here, produces ions with average internal energies higher than the average energy per collision for normal electronvolt CAD experiments on peptides but lower than the energies of the high-energy tail associated with kiloelectronvolt CAD.[34,36] The experimental results presented above show that **w** ions, and a limited number of **d** ions, are produced in SID experiments but they are not as dominant in these SID spectra as in kiloelectronvolt CAD spectra, in agreement with our expectations based on the bond order values and the internal energy distributions associated with these activation methods.

CONCLUSIONS

The results presented above show that surface-induced dissociation provides sufficient structural information to assign the amino acid sequence of many peptides. In general, the relative abundances of low-mass fragment ions increase with increasing collision energy and the parent ion relative abundance decreases with increasing collision energy. The results show that predicted **w** ions are generally detected in surface-induced dissociation spectra, while predicted **d** ions are detected in only a few cases. Additional studies are in progress to determine the conditions needed to form the **d** ions, to evaluate processes that may be competing with **d** ion formation, to evaluate SID fragmentation of fixed charge derivatives, and to better understand the influence of the ion *formation* method on the SID spectra.

MNDO bond order calculations on model compounds **I** and **II**, their singly protonated forms, and selected fragmentation products form the basis for a theoretical model that effectively describes fragmentation of protonated peptides. Several conclusions can be reached: (i) The protonation has a local effect; only the bond orders of bonds α, β, and γ to the protonation site change considerably upon protonation. (ii) Charge-remote backbone cleavages can be modeled by neutral peptides. The weakest bonds in the neutral molecules are the carbon–carbon bonds of the backbone, the cleavage of which leads to $\mathbf{a}_n + 1$ ions if the remote charge is located N-terminal to the cleavage site. With the remote charge at the carboxy terminus, cleavage of the same C–C bond could lead to a **z** + 1 ion via preferred loss of NHCO and subsequent side-chain cleavage would lead to a **w** ion. (iii) Protonation on the amide nitrogen atom leads to a significant weakening of the amide bond (by about 30%). Accordingly, the cleavage of this bond, which can lead to the formation of **b**, **y**, and **a** ions is preferred energetically. (iv) Protonation on the amide oxygen makes the amide C(OH)–N bond stronger; therefore the formation of **b**, **y**, and **a** fragment ions is less likely from this form. (v) N···H···N-type hydrogen bridges leave the amide bond weaker, whereas O···H···O-type bridges makes it stronger; presumably the latter forms have no significant effect on amide bond cleavage as compared with the amide N-protonated structure. (vi) Charge-remote backbone cleavage, followed by side-chain cleavage, is less favorable than the cleavage of the amide bond of a nitrogen-protonated amide, in agreement with experimental observations.

The results described above do not mean that only the amide N or O is protonated or that fragmentation occurs only from amide-protonated forms. The bond order values and SID results can be used in conjunction with CAD data from the literature to support the increasingly popular idea that different protonated forms of a given peptide are precursors of the myriad types of fragment ions detected in MS/MS experiments. In other words, molecules protonated at different sites contribute to the fragmentation spectra to various extents depending on the activation method and sequence involved. Consider, for example, an arginine-containing peptide with a large percentage of the protonated molecules existing as the arginine-protonated structure and a smaller percentage protonated at various amide nitrogens. It is possible that high-energy CAD probes the main (arginine-protonated) population of ions by causing homolytic cleavage leading to dominant **d** and **a** ions via **a** + 1 precursors (e.g., substance P[25]), whereas low-energy CAD (which deposits a low average energy per collision) leads only to fragmentation of the smaller population that consists of amide-protonated forms. Low-energy and high-energy CAD thus lead to

different but useful sequence information, and the techniques are probably best described as complementary. Both CAD and SID results are clearly influenced by the presence of basic groups and studies of fixed-charge derivatized peptides and peptides with basic residues will continue to play a role in elucidating peptide fragmentation mechanisms.

ACKNOWLEDGMENT

We thank Professor Donald F. Hunt for the use of the triple–quadrupole instrument and Dr. Pat Griffin for obtaining several low-energy CAD spectra. This work was supported by the Office of Naval Research, the Thomas F. and Kate Miller Jeffress Memorial Trust, the Society for Analytical Chemists of Pittsburgh, and the Fisons/American Society for Mass Spectrometry Research Award.

RECEIVED for review February 16, 1993. Accepted June 29, 1993.[•]

[•] Abstract published in *Advance ACS Abstracts,* August 15, 1993.